Journal of Food Safety and Food Quality
Archiv für Lebensmittelhygiene

J. Food Saf. Food Qual. **2026**; 77(4): 52383
https://doi.org/10.31083/JFSFQ52383

Original Research

Fabrication and Characterization of Esterified Corn Starch/Chitosan Composite Active Films Incorporated With Mint Extract for Mutton Preservation

Yonghua Bao[1,*], Xiaohong Zhou[1,2], Sudan Ye[1], Chunhui Fu[1,2], Jinfeng Zhang[1]

[1]School of Food and Health, Zhejiang Institute of Economics and Trade, 310018 Hangzhou, Zhejiang, China
[2]Food Inspection Center, Zhejiang Institute of Economics and Trade, 310018 Hangzhou, Zhejiang, China
*Correspondence: byh@zjiet.edu.cn (Yonghua Bao)

Academic Editor: Corinna Kehrenberg
Submitted: 29 March 2026 Revised: 7 June 2026 Accepted: 25 June 2026 Published: 18 August 2026

Abstract

Background: This study developed a novel chitosan (CS)–mint extract (ME)–esterified corn starch (ECS) (CS–ME–ECS) active film to preserve chilled mutton. **Methods:** Using solvent casting, composite films were fabricated with ECS as the continuous matrix, CS as a structural copolymer, and ME as a bioactive agent. **Results:** Structural characterizations via scanning electron microscopy (SEM), Fourier transform infrared (FTIR), and X-ray diffraction (XRD) confirmed excellent interfacial compatibility among these components, thereby synergistically enhancing the overall physicochemical performance of the biocomposite. Notably, the active film exhibited remarkable surface hydrophobicity with a water contact angle of 102.8°, thereby establishing an effective moisture barrier against microbial proliferation. During packaging trials for chilled mutton, the CS–ME–ECS film effectively mitigated oxidative and microbial deterioration, maintaining significantly lower levels of Total Volatile Basic Nitrogen (TVB-N) and Thiobarbituric Acid Reactive Substances (TBARS) ($p < 0.05$) compared to traditional storage, thereby successfully prolonging the shelf life of the meat at 4 °C to 15 days. Additionally, the polymer network was highly susceptible to natural decomposition, with approximately 80% mass loss in soil within 7 days. **Conclusions:** Ultimately, these robust structural, functional, and eco-friendly attributes highlight the strong potential of the CS–ME–ECS film as a sustainable alternative active packaging material for meat preservation.

Keywords: chitosan; anti-bacterial agents; food preservation; food packaging; plant extracts; meat

1. Introduction

Although recognized as an indispensable source of dietary protein, fresh meat is intrinsically highly perishable. The abundant moisture and nutrient-rich muscle matrix create an ideal medium for rapid microbial proliferation and biochemical deterioration during post-slaughter handling and storage [1,2]. To effectively delay these adverse quality alterations and extend commercial shelf life, various preservation interventions have been widely implemented in the food industry. These strategies conventionally rely on temperature control (e.g., refrigeration and freezing), emerging non-thermal physical treatments (such as ultra-high pressure and ionizing radiation), and the incorporation of exogenous chemical preservatives like citric and ascorbic acids [3]. However, the aforementioned methods involved high costs, sophisticated equipment, and potential risks [4]. In comparison, biodegradable films containing bioactive substances, such as plant extracts or essential oils, have garnered considerable attention for their dual functionality in antimicrobial and antioxidant properties [5,6]. The application of these functional packaging matrices has proven highly advantageous in delaying meat spoilage, thereby prolonging commercial shelf life and sustaining overall product integrity [7].

Driven by the escalating demand for sustainable packaging alternatives, starch has garnered tremendous attention owing to its universal availability, affordability, and inherent biodegradability [8]. Nevertheless, the practical implementation of native starch films is substantially impeded by their inferior mechanical profile and limited functional versatility [9]. To circumvent these inherent drawbacks and broaden the application potential of starch-based matrices, current interventions conventionally rely on either the physicochemical tailoring of the polymeric backbone or the formulation of biocomposites with complementary additives [10]. To maximize the synergistic benefits of these approaches, this study concurrently deployed both modification strategies, aiming to engineer a robust starch-based film with significantly upgraded mechanical strength and diverse functional attributes. Chitosan was considered a highly promising biopolymer due to its biodegradability, environmental friendliness, and excellent film-forming characteristics [11].

Consequently, chitosan was co-blended as a fundamental structural skeleton to formulate the starch-based composite matrices [10]. To further functionalize these biopolymers for active packaging, the integration of exogenous bioactive substances has proven highly advantageous in delaying food spoilage. Specifically, mint extract (ME)

emerges as a robust candidate for this purpose. Its naturally enriched phenolic profile confers exceptional antioxidant capabilities, rendering it highly effective in mitigating oxidative deterioration [12,13].

In this study, chitosan (CS)–mint extract (ME)–esterified corn starch (ECS) (CS–ME–ECS) composite film was prepared using the cast film-forming method. To elucidate the microstructural configurations and intermolecular compatibilities, the prepared CS–ME–ECS composite was systematically characterized via scanning electron microscopy (SEM), Fourier transform infrared (FTIR), X-ray diffraction (XRD), and X-ray photoelectron spectroscopy (XPS). Concurrently, the fundamental physicochemical properties including mechanical durability, moisture affinity, and swelling behavior were comprehensively evaluated. Ultimately, the antimicrobial efficacy and freshness preservation capacity of this functionalized biopolymer were monitored during practical meat storage applications. These systematic investigations aimed to provide a reliable theoretical basis and verify the immense potential of this biodegradable chitosan-based system as a sustainable alternative for green food packaging.

2. Experimental Section

2.1 Materials

Fresh mutton (*Ovis aries*) and raw mint (*Mentha haplocalyx* Briq.) leaves were locally sourced from a commercial meat facility (Yijia Agricultural Products Limited, Huzhou, China) and a regional agricultural market in Hangzhou, China, respectively. Chitosan (CS, ≥95%, analytical purity (AR)) and acetic acid solution (≥99.5%, AR) were provided by Macklin Biochemical Co. (Shanghai, China). Corn starch was procured from Jindichao Food Co., Ltd. (Guangdong, China). Zeye Biotechnology Co., Ltd. (Shanghai, China) served as the provider for D-sorbitol (98%, AR). Succinic anhydride (SA, 97%, AR) was obtained via Honghu United Chemical Products Co., Ltd. (Beijing, China). Routine biological consumables were acquired from a local scientific vendor. Unless otherwise specified, all other chemicals utilized herein met AR standards and were applied strictly as received.

2.2 Preparation of Esterified Corn Starch

ECS was synthesized according to the study of Qiu et al. [14], with some modification. An aqueous suspension was first formulated by vigorously dispersing 40 g of corn starch into 60 mL of distilled water. Upon adjusting the system to a stable pH of 8.5 using a 3% (w/v) NaOH solution, the mixture was continuously agitated at ambient temperature for 30 min. 4% (w/v) SA was incorporated into the suspension, during which the system's alkalinity was maintained via the dropwise addition of NaOH. After a 3-h esterification process, the reaction was quenched by reducing the pH to 6.5 using 1% (w/v) HCl. The resulting precipitates were recovered through filtration, washed thrice with distilled water, vacuum-dried at 37 °C for 24 h, and mechanically pulverized through a sieve (100 mesh).

2.3 Preparation of Mint Extract

Briefly, 100 g of leaves underwent an initial aqueous extraction by refluxing in 1000 mL of distilled water for 1 h, followed by cooling and straining through cheesecloth. The retained biomass was subjected to a secondary 1.5-h reflux. The pooled liquid fractions were then centrifuged for 15 min. Ultimately, the collected supernatant was concentrated utilizing a rotary evaporator, and the recovered extracts were completely dehydrated into fine powders by freeze-drying, which were preserved at 4 °C for subsequent applications.

2.4 Fabrication of CS-ME-ECS Films

The composite packaging films were fabricated via a modified solvent casting method [10]. Initially, a 2% (w/v) CS solution was formulated by dispersing the powder in acetic acid solution (1%, v/v) under continuous magnetic agitation at 75 °C for 8 h. Upon cooling to ambient temperature, predetermined mass gradients of ECS (1.0% to 3.0% (w/v)) were blended into the biopolymer matrix. This procedure was immediately followed by the dropwise addition of mint extract (ME) at varying concentrations ranging from 0.4% to 1.2% (w/v). Subsequently, 1.8 g of D-sorbitol was incorporated to plasticize the network, and the ternary mixture was agitated for an additional 30 min to ensure complete homogenization. To cast the films, 15 mL aliquots of the respective homogeneous suspensions were poured onto glass Petri dishes (9 cm × 9 cm) and dried in a ventilated oven at 37 °C for 12 h (Scheme 1). The dried composite specimens with varying formulation ratios were stored in desiccators for subsequent property evaluations to screen for the most suitable matrix for mutton preservation.

2.5 Characterization of Active Films

Spectral data of the films were gathered using a Nicolet iS50 Fourier Transform Infrared spectrometer (FTIR, Thermo Fisher, USA). The surface elemental compositions and internal crystalline architectures were systematically evaluated utilizing X-ray photoelectron spectroscopy (XPS, Thermo Fisher, USA) and a D2 PHASER X-ray diffractometer (XRD, Bruker, Germany), respectively. Microstructural morphology was visualized with an EVO-LS10 scanning electron microscope (SEM, Carl Zeiss AG, Germany) operating at an accelerating voltage of 5 kV. Prior to this observation, the specimens underwent cryogenic fracture in liquid nitrogen followed by gold sputter-coating. The captured micrographs were subsequently processed via ImageJ software (version 1.54g, National Institutes of Health, Bethesda, MD, USA) to quantify the structural porosity. DSA100S drop shape analyzer (Biolin Science and Technology Co., Ltd., Gothenburg, Sweden) monitored the hydrophilicity. Thermal degradation behavior

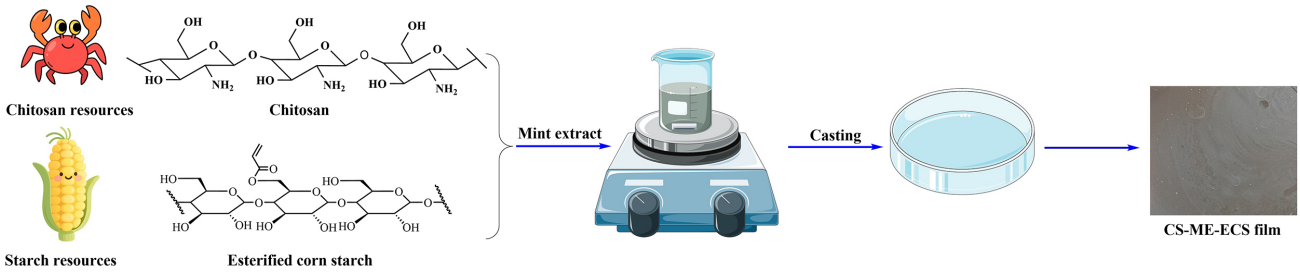

Scheme 1. Preparation process of CS-ME-ECS composite film. CS, chitosan; ME, mint extract; ECS, esterified corn starch.

and phase transitions were simultaneously tracked using a HITACHI thermogravimetric/differential thermal analyzer (TGA, TG/DTA7200, Japan) with calibrated DSC heat flow output.

2.6 Determination of Mechanical and Physicochemical Properties

The film thickness was calculated as the mean of five random spatial measurements using a digital micrometer (Mitutoyo Absolute Tester, Tokyo Sangyo Co., Ltd., Japan). For mechanical evaluations, the samples were precisely tailored into uniform rectangular strips (10 mm × 40 mm). The tensile strength (TS) and elongation at break (EAB) were assessed at ambient temperature utilizing a TMS-Pilot texture analyzer (FTC, Leesburg, VA, USA). The initial grip spacing was rigidly fixed at 10 mm with a constant crosshead extension rate of 20 mm/min.

The opacity of the films was determined following the protocol established by Simsek et al. [15]. The specimens were precisely tailored into uniform rectangular strips (4.5 cm × 1.2 cm) and mounted securely against the internal wall of a quartz cuvette. A UV-vis spectrophotometer (Genesys50, Thermo Fisher Scientific, Waltham, MA, USA) subsequently recorded the sample absorbance at a fixed wavelength of 600 nm. The acquired optical readings were then substituted into Eqn. 1 to calculate the final opacity value:

$$\text{Opacity} = \frac{\text{absorbance 600 nm}}{\text{sample thickness(mm)}} \tag{1}$$

2.7 Determination of Moisture Content (MC) and Swelling Rate (SR)

The MC was quantified gravimetrically by dehydrating the film in a hot-air oven at 105 °C until a consistent dry mass was reached. The percentage of MC was calculated according to Eqn. 2 [16] :

$$\%\ \text{MC} = \left(\frac{\text{m} - \text{M}}{\text{m}}\right) \times 100 \tag{2}$$

where m and M represent the pre-drying initial weight and the post-drying constant mass, respectively.

SR was determined by adapting the procedure of Wei et al. [10]. The film specimens were completely submerged in distilled water and allowed to swell at a controlled temperature of 25 °C for 24 h. Subsequently, the hydrated samples were retrieved. Free water adhering to the exterior was gently blotted dry using filter paper prior to weighing. The SR was determined by applying Eqn. 3:

$$\%\ \text{SR} = \left(\frac{\text{W}_1 - \text{W}_0}{\text{W}_0}\right) \times 100 \tag{3}$$

where W_0 and W_1 represent the initial dehydrated mass and the final hydrated mass, respectively.

2.8 Soil Burial Degradation (SBT) of the Film

To evaluate the natural biodegradability of the composite matrix, a simulated SBT was performed [17,18]. Uniform square specimens (30 mm × 30 mm) were precisely pre-weighed and embedded at a depth of 5 cm within plastic containers holding natural garden soil. Adequate hydration for microbial degradation was ensured by spraying 5 mL of tap water daily. Throughout the testing period, the surrounding environment was rigidly maintained at room temperature with constant humidity. The degraded film fragments were excavated at assigned incubation intervals of 1, 3, 5, and 7 days. Residual soil particles adhering to the matrix were gently detached using a soft brush. The samples were desiccated in an oven at 40 °C for 20 min to achieve a constant weight. The soil degradation rate was then computed based on Eqn. 4:

$$\%\ \text{Soil degradation} = \left(\frac{\text{IW} - \text{DeW}}{\text{IW}}\right) \times 100 \tag{4}$$

where IW and DeW denote the original mass of the intact specimen and its residual weight recorded post-burial, respectively.

2.9 The Application of Film in the Preservation of Mutton

In a sterile environment, after the skin, visible fat, and connective tissues were carefully removed, the fresh lean mutton (*Ovis aries*) was cut into uniform blocks with an average weight of approximately 50 g. The samples were then divided into two groups. Group NA served as the blank control without any packaging treatment. For the experimental group (Group CS-ME-ECS), each mutton block was individually and entirely wrapped with a piece of the selected optimal active film (dimensions: 9 cm × 9 cm) covering its surface. Subsequently, all samples from both groups were placed into separate 100 mL sterile beakers, sealed within sterile polyethylene bags, and stored in a refrigerator at 4 °C. The evaluation of the meat quality parameters was conducted at 1, 3, 5, 7, 9, 11, 13, and 15 days. Under aseptic conditions, samples were analyzed for chemical and microbiological properties.

2.9.1 pH and Total Viable Count (TVC)

For pH measurements, 5 g aliquots of minced meat were vigorously blended with 50 mL of distilled water at ambient temperature for 30 min. The stabilized acidity of the resulting homogenates was directly captured using a digital pH meter (PHS-3E, Leici, China). The TVC of the mutton samples was quantified through the standard plate count method based on the GB 4789.2-2022 standards and procedures established by Qi et al. [19]. Primary bacterial suspensions were formulated by transferring 25 g of the tissue into sterile sealed bags containing 225 mL of physiological saline for mechanical homogenization. Sequential tenfold dilutions derived from this mixture were subsequently inoculated onto plate count agar. Following a 48 h incubation phase at 37 °C, the visible colonies were enumerated to calculate the TVC expressed as log CFU/g.

2.9.2 Total Volatile Basic Nitrogen (TVB-N)

In accordance with the Chinese Standard (GB 5009.228-2016), TVB-N was quantified via a steam distillation protocol [20]. The distillation was executed employing an automated Kjeldahl analyzer (Kjeltec 8400, FOSS, Denmark). The final results, expressed as mg/100 g of fresh meat, were computed based on the exact titration volume of 0.1 mol/L HCl.

2.9.3 Thiobarbituric Acid Reactive Substances (TBARS)

The accumulation of TBARS within the mutton samples was monitored using a UV-vis spectrophotometer. The analytical results are presented as mg MDA/kg mutton. Detailed procedures for the TBARS extraction, colorimetric reaction, and calculation formula are appended in **Supplementary Material (S1)**.

2.9.4 Statistical Analysis

All experimental assays were performed three times, and the results were expressed as the mean ±SD. Statistical evaluations were conducted via analysis of variance coupled with Duncan's multiple range test utilizing SPSS 29.0 (IBM Corp., Armonk, NY, USA), significance was set as $p < 0.05$. Graphs were plotted employing Origin 2025b software (OriginLab Corporation, Northampton, MA, USA).

3. Results and Discussion

3.1 Assessment of Physical, Optical, and Mechanical Properties

The effects of varying ME and ECS contents on their physical properties (including thickness, moisture content, and swelling ratio), optical property (opacity), and mechanical properties (tensile strength and elongation at break) were systematically investigated (**Supplementary Fig. 1**)

According to the holistic assessment of these physicochemical properties, the composite film containing 0.8 g of ME and 2.0 g of ECS exhibited the optimal overall performance. Therefore, this specific optimal formulation was selected as the representative film to track the deterioration dynamics of chilled mutton across the designated storage timeframe. Further detailed data and analyses regarding these parameters are provided in the **Supplementary Material**.

3.2 FTIR Analysis

To elucidate the structural alterations and intermolecular compatibilities among the film constituents, FTIR spectroscopy was conducted (Fig. 1A). In the spectrum of pure ECS, a distinct absorption signal emerged at 1715 cm^{-1}, which was assigned to the C=O stretching vibrations, verifying the successful grafting of ester carbonyl groups onto the starch backbone [10]. For the ME spectrum, prominent bands at 2940 cm^{-1} and 1652 cm^{-1} were ascribed to the aliphatic C–H and carbonyl (C=O) stretching vibrations, respectively, alongside a broad O–H stretching band near 3380 cm^{-1} reflecting the abundance of menthol [12]. The CS spectrum presented a characteristic broad region spanning 3500–3000 cm^{-1}, resulting from the overlapping stretching vibrations of –OH and –NH groups [21]. The CS-ME-ECS composite film retained the fundamental skeletal peaks of its precursors. Nevertheless, discernible spectral displacements and intensity variations were detected, specifically the broadening and shifting of the overlapping –OH/–NH domain (3500–3000 cm^{-1}), the diminished resolution of the Amide II band (1590 cm^{-1}), and the intensified C–O stretching signals (1240–1000 cm^{-1}). Such band displacements typically occur when new non-covalent interactions are established [10]. These alterations demonstrated the development of robust intermolecular hydrogen bonds between the amino/hydroxyl groups of the CS matrix and the active carbonyl/hydroxyl sites of ECS and ME, facilitating the excellent structural integration of the ternary system.

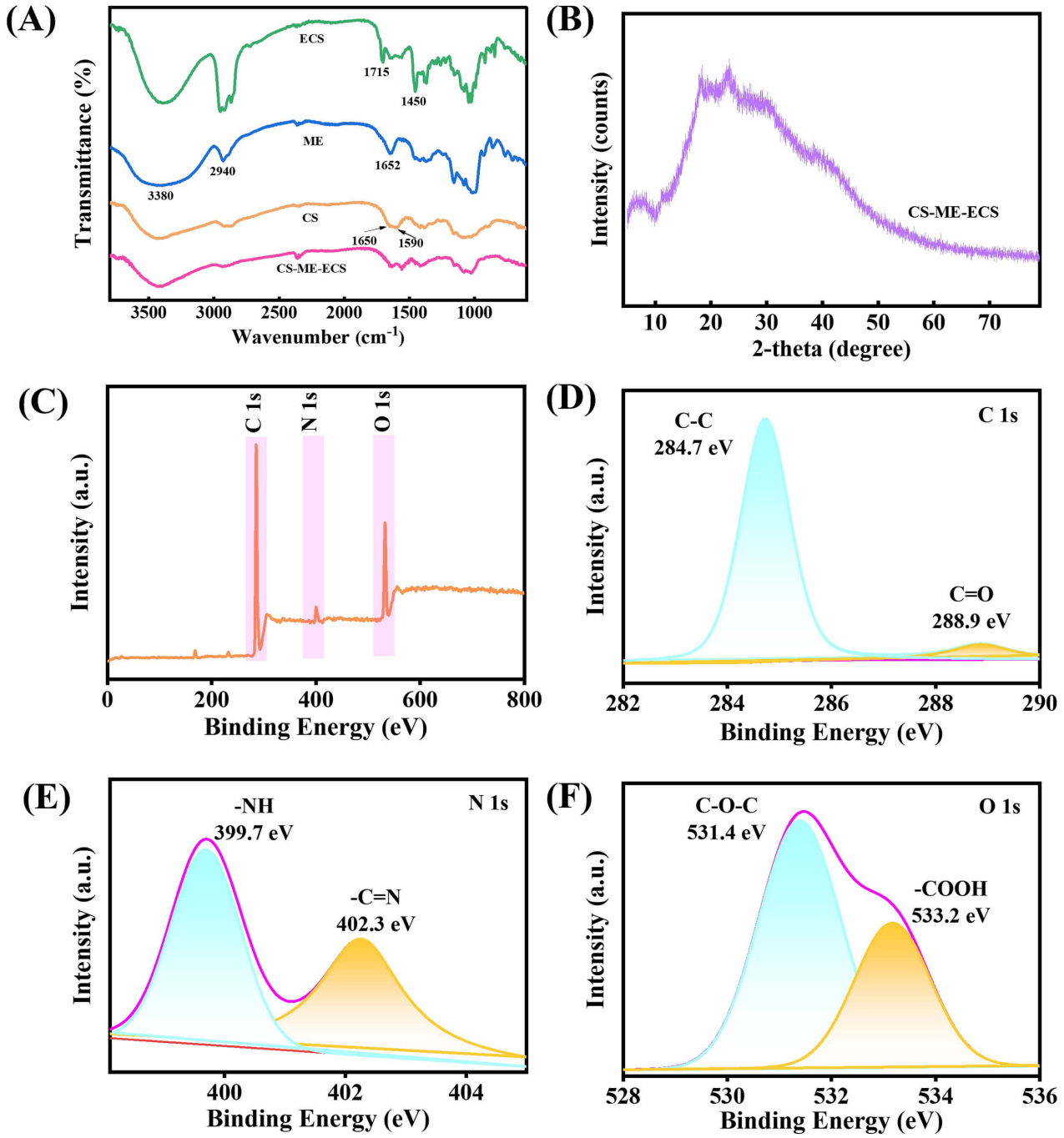

Fig. 1. Structural and chemical composition analysis of the films. (A) FTIR spectra of ECS, ME, CS, and the CS-ME-ECS composite film; (B) XRD pattern of the CS-ME-ECS film; (C) XPS full spectrum of the CS-ME-ECS composite film; High-resolution XPS spectra of (D) C 1s, (E) N 1s, and (F) O 1s for the composite film. FTIR, Fourier transform infrared spectroscopy; XRD, X-ray diffraction; XPS, X-ray photoelectron spectroscopy.

3.3 XRD Analysis

As shown in Fig. 1B, broad diffraction peaks around $2\theta = 18.5–23.2°$ were observed, which are characteristic of the amorphous or semi-crystalline nature of the composite films. The presence of these broad, diffuse scattering patterns instead of sharp crystalline peaks indicates that the original ordered crystalline structures of starch and chitosan were largely disrupted during the gelatinization and blending processes, resulting in a predominantly amorphous matrix with a dense intermolecular network [22]. The absence of sharp crystalline peaks and the presence of broad, diffuse scattering patterns were primarily attributed to the for-

mation of hydrogen bonds and other intermolecular interactions among CS, ME, and ECS, leading to enhanced molecular disorder and improved compatibility between the different phases [10,23].

3.4 XPS Analysis

The XPS full spectrum demonstrated the prominent existence of carbon (C 1s), nitrogen (N 1s), and oxygen (O 1s) within the polymeric matrix (Fig. 1C). Specifically, the high-resolution C 1s spectrum (Fig. 1D) was deconvoluted into two distinct signals at 284.7 eV and 288.9 eV, assigned to the C–C and C=O moieties, respectively [24]. For the N 1s region (Fig. 1E), the binding energies detected at 399.7 eV and 402.3 eV corresponded well with the –NH and C=N linkages. Furthermore, the O 1s fine spectrum (Fig. 1F) was fitted with two components at 531.4 eV and 533.2 eV, attributable to the C–O–C and –COOH groups. Collectively, these spectral characteristics convincingly corroborated the successful incorporation of ester and carboxyl functionalities within the composite architecture.

3.5 Thermal Stability Analysis

As depicted in Fig. 2A, the mass loss underwent a typical three-step decomposition profile. The initial weight reduction (Phase I, <245.51 °C) was principally driven by the evaporation of free moisture and weakly attached water within the matrix. Subsequently, a drastic thermal degradation occurred between 245.51 and 344.74 °C (Phase II) with a dominant mass loss of approximately 70%. This sharp decline was fundamentally ascribed to the thorough depolymerization and pyrolytic decomposition of the principal polymeric backbones (CS and ECS), alongside the volatilization of ME [25]. Ultimately, during Phase III (>344.74 °C), the decomposition rate significantly decelerated, corresponding to the progressive carbonization of the remaining residues. Concurrently, the DSC curve (Fig. 2B) exhibited a prominent endothermic peak at 105.71 °C, confirming the vaporization of trapped H_2O and other volatile molecules. Furthermore, a distinct exothermic transition observed near 313.03 °C signified the severe structural disintegration of the composite framework.

3.6 SEM Analysis

Microstructural topography of the CS-ME-ECS packaging was visually captured using SEM (Fig. 3). The micrographs revealed a continuous and compact matrix containing rounded granular domains (9.74 ± 2.96 μm), which were attributed to ECS particles partially embedded within the chitosan network. These granules exhibited rough and irregular morphologies with occasional surface porosity, consistent with previous reports [14]. It was speculated that ME, owing to its abundant surface hydroxyl groups, could form extensive hydrogen bonds with the amino groups of CS, thereby enhancing the interfacial adhesion. This morphological observation is fundamentally supported by the interpolymer interactions and amorphous characteristics inferred from the previous FTIR and XRD analyses. Specifically, the robust non-covalent interactions (primarily hydrogen bonding) among the multiple components effectively restrict the mobility of the polymer chains and disrupt the ordered crystalline domains, which ultimately facilitates the formation of a highly compatible, predominantly amorphous matrix with a dense and continuous network [10,22,26].

3.7 Hydrophilicity Analysis

As shown in Fig. 4, the initial water contact angle (WCA) value for the CS–ME–ECS composite was recorded at 102.8°, which signifies a distinctly hydrophobic character (>100°) [17]. This elevated contact angle demonstrated that the simultaneous incorporation of ME and ECS reduced the hydrophilicity of the polymeric matrix, corroborating prior study on functionalized active films [27]. Furthermore, the time-dependent WCA was evaluated by continuously tracking the droplets at 10 s and 20 s. The corresponding results revealed that the WCA values underwent merely negligible declines as time progressed, thereby maintaining relatively excellent water resistance. This sustained surface hydrophobicity would substantially enhance the practical applicability of these composite films in moist packaging environments.

3.8 Biodegradability of the Film

To evaluate environmental sustainability, the biodegradation profile and the corresponding degradation rate of the composite films were monitored via a 7-day soil burial assay (Fig. 5). During this period, all specimens experienced progressive weight reduction, culminating in a remarkable maximum degradation of 80%, which verified their excellent susceptibility to natural decomposition. This pronounced structural disintegration is fundamentally driven by the synergistic action of ubiquitous soil microflora and environmental moisture, which effectively catalyze the cleavage of polymeric backbone linkages [26,28]. Consequently, such outstanding eco-friendly degradability highlights the immense potential of these materials as sustainable alternatives for active packaging.

3.9 Practical Application of Active Films in Mutton Preservation

3.9.1 pH Analysis

The pH profiles of both the NA and CS-ME-ECS samples (Fig. 6A) presented a transient decline from day 1 to day 3, succeeded by a continuous upward trend. Notably, the CS-ME-ECS treatment maintained significantly suppressed pH levels relative to the bare NA control at each sampling point ($p < 0.05$), verifying that the active packaging effectively retarded the pH escalation during storage. The initial pH drop is fundamentally driven by lactic acid accumulation generated via the anaerobic degradation of in-

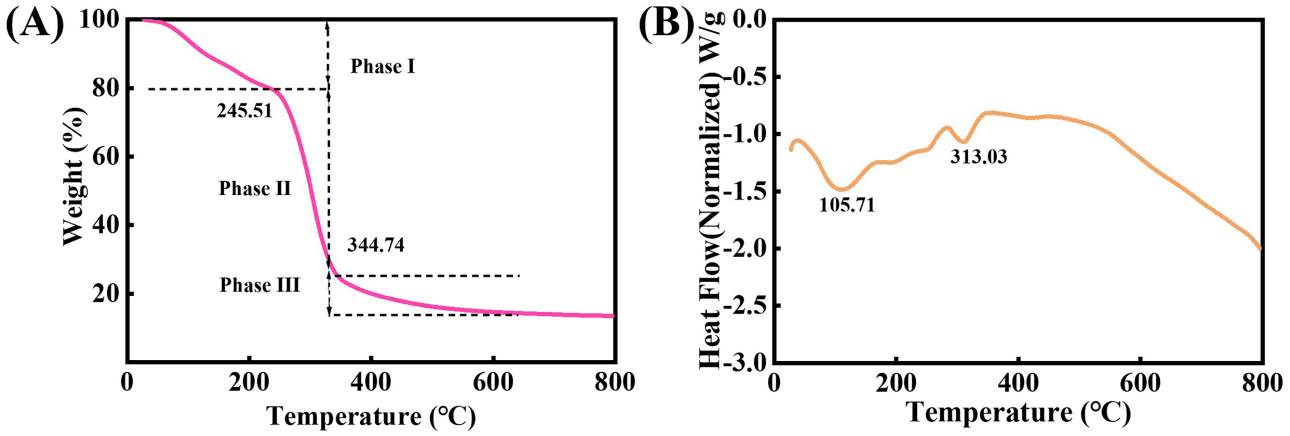

Fig. 2. Thermal stability analysis. (A) TGA and (B) DSC thermograms of the CS-ME-ECS composite films. TGA, Thermogravimetric analysis; DSC, Differential scanning calorimetry.

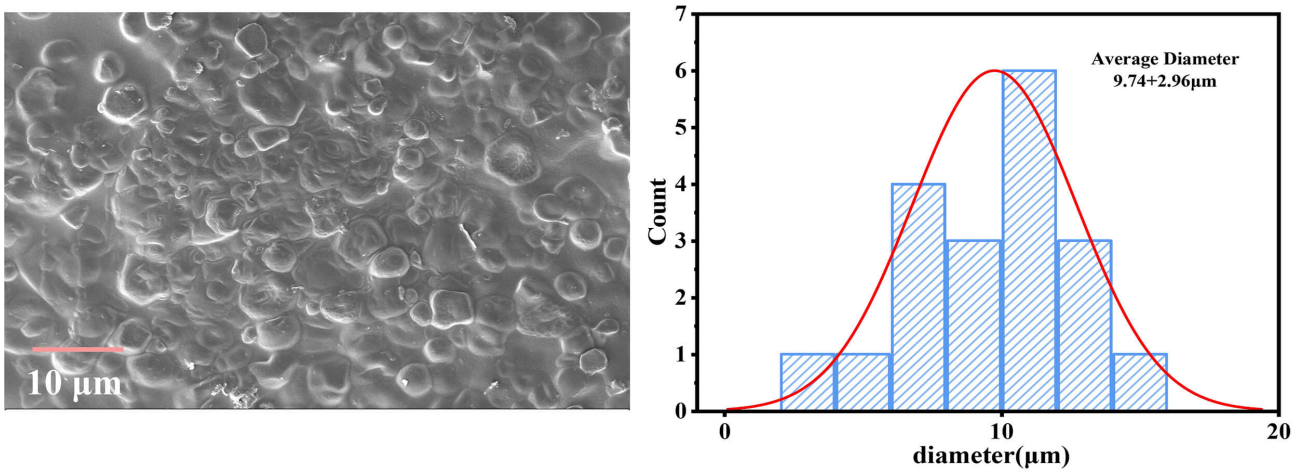

Fig. 3. SEM image of the CS-ME-ECS film and the size distribution of the observed particulate regions. SEM, scanning electron microscopy; Scale bar, 10 μm.

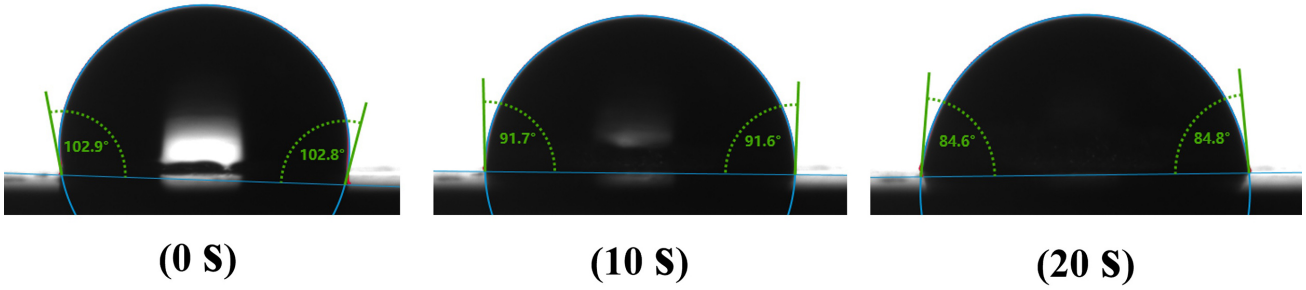

Fig. 4. The water contact angle of CS–ME–ECS films.

tramuscular glycogen stores [29]. Conversely, the subsequent pH increase is ascribed to the extensive degradation of meat proteins during prolonged storage, which ultimately produces abundant alkaline nitrogenous metabolites (e.g., TVB-N) [1].

3.9.2 TVB-N Analysis

In accordance with the Chinese National Standard (GB 2707-2016), the acceptable threshold of TVB-N for fresh meat is specified to be less than 15 mg/100 g. As illustrated in Fig. 6B, an upward trend in TVB-N levels was observed across all mutton samples during the chilled storage period. However, the samples enveloped with the

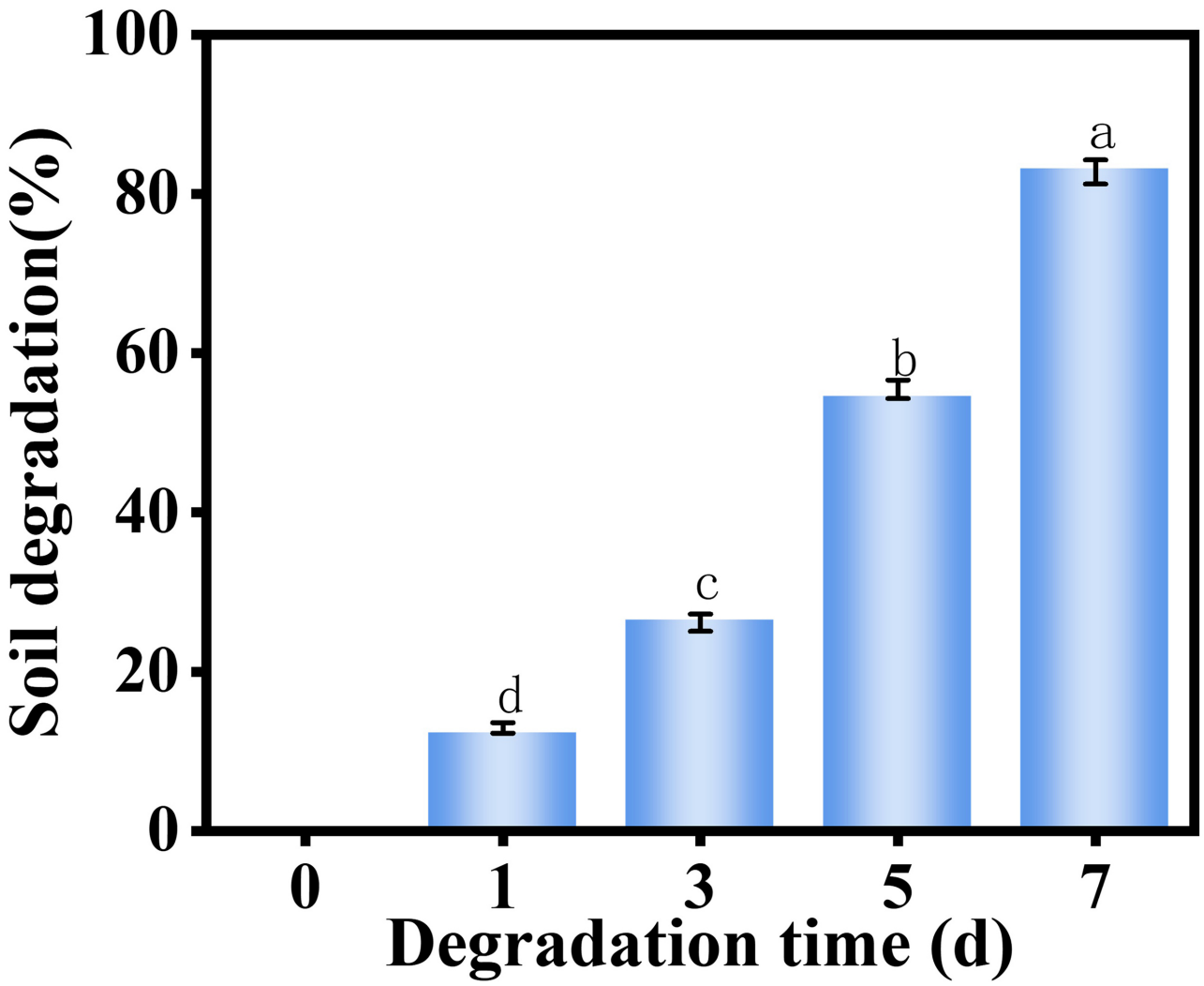

Fig. 5. Soil degradation within 7 d. Different letters for the same test parameter indicate significant differences among different groups ($p < 0.05$).

CS-ME-ECS film exhibited a substantially suppressed accumulation rate compared to the uncoated NA control ($p < 0.05$). Specifically, the TVB-N value of the NA group surged sharply from 6.14 to 28.35 mg/100 g, exceeding the acceptability limit on day 9. Conversely, the TVB-N content in the CS-ME-ECS group merely elevated from 4.89 to 11.76 mg/100 g over the 15 days of storage, successfully keeping the mutton well below the established spoilage limit. This significantly decelerated production of TVB-N in the packaged samples can be fundamentally ascribed to the robust antibacterial efficacy contributed by the mint extract and chitosan matrix. These biologically active ingredients effectively repressed the proliferation of spoilage microorganisms, thereby mitigating microbial-mediated protein hydrolysis and the subsequent generation of volatile alkaline metabolites [3,21,29,30]. Consequently, the application of the CS-ME-ECS active packaging successfully retarded protein degradation, prolonging the viable storage duration of chilled mutton from 9 days to at least 15 days.

3.9.3 TBARS Analysis

As depicted in Fig. 6C, all samples experienced a progressive escalation in TBARS values throughout the 15-day chilled storage. Nevertheless, the CS-ME-ECS composite film remarkably suppressed this oxidative deterioration compared to the NA control ($p < 0.05$). By day 13, TBARS accumulation in the unprotected control surged to 1.33 mg/kg. In contrast, the CS-ME-ECS wrapping effectively suppressed this oxidative marker to a mere 0.53 mg/kg. This inhibitory effect on lipid oxidation was primarily attributed to the synergistic antioxidative action of the bioactive components within the composite film, coupled with its enhanced oxygen barrier capacity. Specifically, the abundant phenolic compounds enriched in the mint extract function as potent hydrogen donors, which effectively scavenge lipid free radicals and interrupt the autoxidation chain reactions [23]. Beyond direct radical scavenging, these exogenous phytochemicals engage in extensive intermolecular cross-linking with the host biopolymer

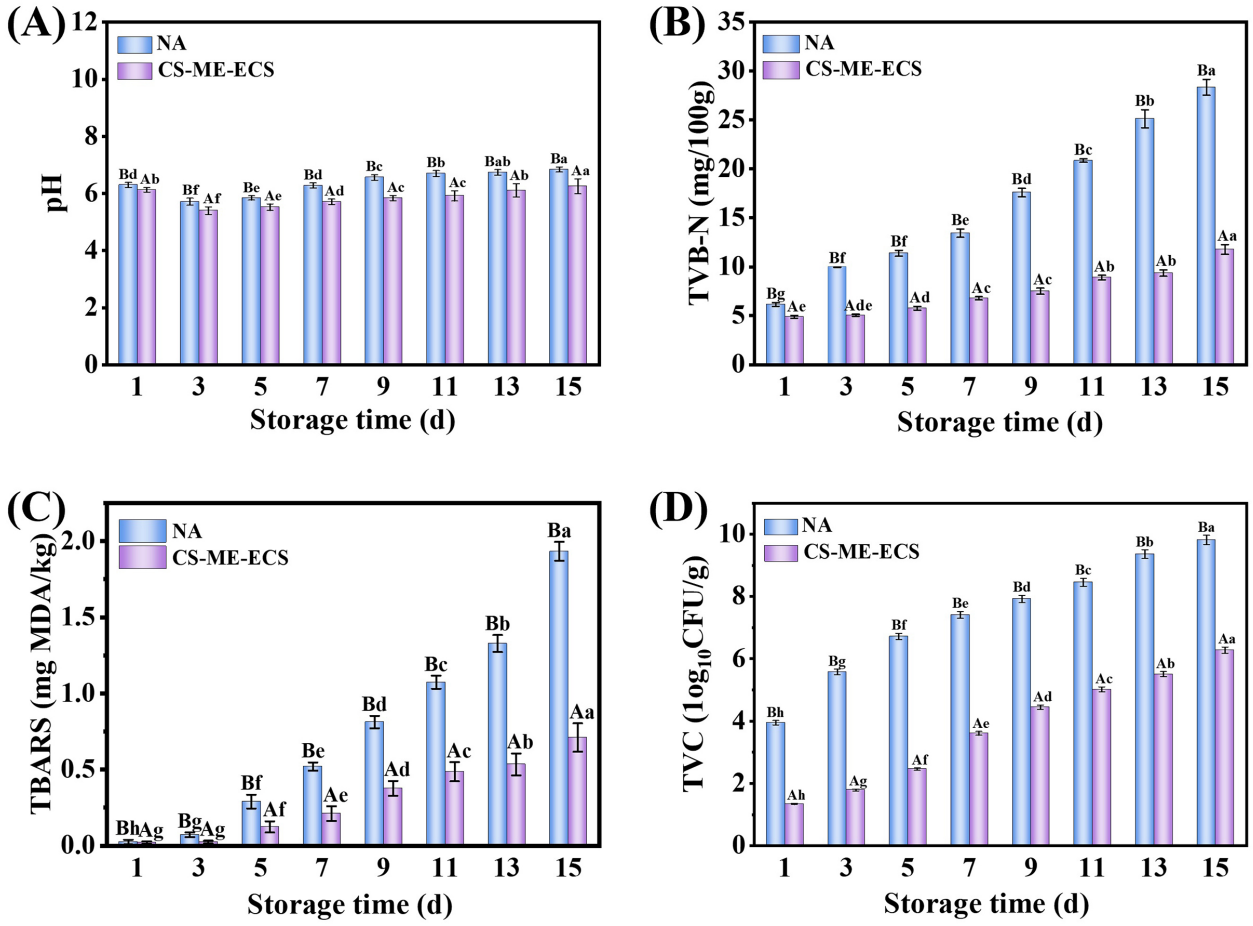

Fig. 6. Quality changes of mutton samples during refrigerated storage. (A) pH; (B) TVB-N; (C) TBARS; and (D) TVC. The significance level was set to $p < 0.05$. The lowercase and uppercase letters in the figure represent the significant differences within the same treatment group across different storage times and between different treatment groups on the same storage day, respectively. NA, No Addition; TVB-N, Total Volatile Basic Nitrogen; TBARS, Thiobarbituric Acid Reactive Substances; TVC, Total Viable Count.

skeleton, which significantly restricts oxygen permeation, acting as a robust physical barrier [17].

3.9.4 TVC Analysis

Bacterial proliferation dynamics depicted in Fig. 6D reveal that the CS-ME-ECS wrapping strongly suppressed microbial growth compared to the unprotected NA samples across the entire testing timeframe ($p < 0.05$). International regulatory guidelines establish a strict upper threshold of 7.00 log CFU/g for the total viable count (TVC) in edible meat products [31]. The TVC of the NA control breached this critical limit by day 7 and underwent rapid subsequent multiplication. Conversely, the functionalized CS-ME-ECS matrix successfully restricted bacterial populations to acceptable safety levels up to day 15. This trend was consistent with the biochemical degradation patterns evidenced by the TVB-N assay. Mechanistically, this superior preservation performance is driven by a synergistic dual-action mechanism. The tightly cross-linked chitosan skeleton initially acts as a robust physical shield against external microbial invasion. Concurrently, the integrated ME exerts potent biocidal effects to continuously inactivate endogenous spoilage organisms [2,32].

3.10 Limitations

Although the developed CS-ME-ECS active packaging exhibits promising properties, certain limitations within this study should be objectively recognized. Primarily, the current composite films were prepared via a laboratory-level solvent casting technique. To meet the demands of commercialization, future studies must transition from laboratory preparation to pilot or full-scale manufacturing processes, aiming to improve cost-effectiveness and operational efficiency. Secondly, the fresh-keeping performance of the active films was solely verified using chilled mutton stored at a specific refrigeration condition (4 °C) for a limited 15-day period. Consequently, subsequent research should incorporate a broader representation of meat products under fluctuating storage temperatures to comprehensively confirm its practical packaging efficacy.

4. Conclusion

In this study, a novel CS-ME-ECS biodegradable composite film was successfully prepared via a standard solvent casting protocol for mutton preservation. Integrating CS as a structural co-polymer and ME as a bioactive agent into the continuous ECS matrix fundamentally upgraded the overall structural profile. Such synergistic blending strongly fortified the mechanical durability and essential physicochemical traits of the composite film. Concurrently, these robust interfacial interactions conferred superior thermal endurance and heightened hydrophobicity to the final packaging material. Furthermore, SEM and FTIR analyses demonstrated that the bioactive components exhibited good compatibility and formed stable cross-linking interactions with the film matrix. Notably, the soil burial tests indicated that the composite film achieved approximately 80% degradation after 7 days, demonstrating its excellent biodegradability. In practical application, compared with the control group, the chilled mutton wrapped with the CS-ME-ECS film significantly delayed the quality deterioration, extending its shelf life over a 15-day storage period at 4 °C. Therefore, the developed active composite film possessed excellent comprehensive properties, making it a highly promising and sustainable packaging material for maintaining the quality and safety of fresh meat.

Availability of Data and Materials

The data mentioned in the article will be available with the corresponding author.

Author Contributions

YB: Writing—review & editing, Writing—original draft, Methodology, Software, Formal analysis, Data curation. XZ: Resources, Methodology, Data curation, Investigation, Validation, Visualization. SY: Supervision, Project administration. CF: Validation, Data curation. JZ: Investigation, Data curation, Formal analysis. All authors contributed to editorial changes in the manuscript. All authors read and approved the final manuscript. All authors have participated sufficiently in the work and agreed to be accountable for all aspects of the work.

Ethics Approval and Consent to Participate

Not applicable.

Acknowledgment

The authors thank Xiaoyong Xu from a local mutton company for providing the fresh mutton.

Funding

This work was supported by "the Fundamental Research Funds for the Provincial Universities", Zhejiang Institute of Economics and Trade (Grant Number: 21SBYB03).

Conflicts of Interest

The authors declare no conflicts of interest.

Declaration of AI and AI-Assisted Technologies in the Writing Process

During the preparation of this work, the authors used Google Gemini in order to check spelling, refine grammar, and improve language fluency in the entire manuscript. After using this tool, the authors reviewed and edited the content as needed and take full responsibility for the content of the publication.

Supplementary Material

Supplementary material associated with this article can be found, in the online version, at https://doi.org/10.31083/JFSFQ52383.

References

[1] Chang W, Liu F, Sharif HR, Huang Z, Goff HD, Zhong F. Preparation of chitosan films by neutralization for improving their preservation effects on chilled meat. Food Hydrocolloids. 2019; 90: 50–61. https://doi.org/10.1016/j.foodhyd.2018.09.026

[2] Xiao L, Lapu M, Cui L, Li J, Wang X, Li X, et al. Impacts of chitosan/pullulan/carvacrol film on the quality and microbial diversity of refrigerated goat meat. Meat Science. 2025; 220: 109704. https://doi.org/10.1016/j.meatsci.2024.109704

[3] Guo Z, Wu S, Lin J, Zheng H, Lei H, Yu Q, et al. Active film preparation using pectin and polyphenols of watermelon peel and its applications for super-chilled storage of chilled mutton. Food Chemistry. 2023; 417: 135838. https://doi.org/10.1016/j.foodchem.2023.135838

[4] Ren B, Wu W, Soladoye OP, Bak KH, Fu Y, Zhang Y. Application of biopreservatives in meat preservation: a review. International Journal of Food Science & Technology. 2021; 56: 6124–6141. https://doi.org/10.1111/ijfs.15307

[5] Song L, Hou F, Yi F, Zhan S, Chen X, Han X, et al. Sustained-release film prepared by incorporation of cinnamon essential oil: Physicochemical properties and application in the preservation of mushroom (Agaricus bisporus). Journal of Stored Products Research. 2024; 105: 102253. https://doi.org/10.1016/j.jspr.2024.102253

[6] Madani Z, Lahreche T, Gasmi K, Bensid A, Benamara RN. Efficacy of warming essential oil emulsions in extending the shelf life of vacuum-packed chicken legs. Journal of Food Safety and Food Quality. 2025; 76: 37401. https://doi.org/10.31083/JFSFQ37401

[7] Cheng J, Velez FJ, Singh P, Cui L. Fabrication, characterization, and application of pea protein-based edible film enhanced by oregano essential oil (OEO) micro- or nano-emulsion. Current Research in Food Science. 2024; 8: 100705. https://doi.org/10.1016/j.crfs.2024.100705

[8] Xia Y, Gao C, Li Y, Meng F, Wang S, Kong F. Investigating the effect of different substitution levels of starch carbamate on composite film properties. Industrial Crops and Products. 2023; 192: 116024. https://doi.org/10.1016/j.indcrop.2022.116024

[9] Liu Q, Gao L, Qin Y, Ji N, Dai L, Xiong L, et al. Incorporation of oxidized debranched starch/chitosan nanoparticles for enhanced hydrophobicity of corn starch films. Food Packaging and Shelf Life. 2023; 35: 101032. https://doi.org/10.1016/j.fpsl.2023.101032

[10] Wei D, Lv S, Liu J, Zuo J, Mu Y, Liu L, et al. Esterification modified corn starch composite with chitosan and PVP

for enhanced mechanical properties and antimicrobial freshness preservation of starch-based films. Reactive and Functional Polymers. 2024; 202: 105991. https://doi.org/10.1016/j.reactfunctpolym.2024.105991

[11] Shahdadi F, Faryabi M, Khan H, Sardoei AS, Fazeli-Nasab B, Goh BH, et al. *Mentha longifolia* Essential Oil and Pulegone in Edible Coatings of Alginate and Chitosan: Effects on Pathogenic Bacteria in Lactic Cheese. Molecules (Basel, Switzerland). 2023; 28: 4554. https://doi.org/10.3390/molecules28114554

[12] Rashid IA, Faisal M, Ahmad A, Afzal A, Khaliq Z, Ashraf MS, et al. Harnessing the antimicrobial potential of natural starch and mint extract in PVA-based biodegradable films against staphylococcus aureus bacteria. Materials Research Express. 2024; 11: 035401. https://doi.org/10.1088/2053-1591/ad1263

[13] Marc Vlaic RA, Mureșan V, Mureșan AE, Mureșan CC, Tanislav AE, Pușcaș A, et al. Spicy and Aromatic Plants for Meat and Meat Analogues Applications. Plants (Basel, Switzerland). 2022; 11: 960. https://doi.org/10.3390/plants11070960

[14] Qiu L, Hu F, Peng Y. Structural and mechanical characteristics of film using modified corn starch by the same two chemical processes used in different sequences. Carbohydrate Polymers. 2013; 91: 590–596. https://doi.org/10.1016/j.carbpol.2012.08.072

[15] Simsek M, Eke B, Demir H. Characterization of carboxymethyl cellulose-based antimicrobial films incorporated with plant essential oils. International Journal of Biological Macromolecules. 2020; 163: 2172–2179. https://doi.org/10.1016/j.ijbiomac.2020.09.075

[16] Shah MAR, Zhang Y, Rehman OU, Zhu F, Kumar S, Hu X, et al. Colorimetric films of carboxymethyl cellulose and sodium alginate incorporating Spirulina extract (phycobiliproteins) and gallic acid for real-time shrimp freshness monitoring. International Journal of Biological Macromolecules. 2025; 309: 143006. https://doi.org/10.1016/j.ijbiomac.2025.143006

[17] Haridevamuthu B, Raj D, Chandran A, Murugan R, Seetharaman S, Dhanaraj M, et al. Sustainable food packaging: Harnessing biowaste of Terminalia catappa L. for chitosan-based biodegradable active films for shrimp storage. Carbohydrate Polymers. 2024; 329: 121798. https://doi.org/10.1016/j.carbpol.2024.121798

[18] La Mantia FP, Ascione L, Mistretta MC, Rapisarda M, Rizzarelli P. Comparative Investigation on the Soil Burial Degradation Behaviour of Polymer Films for Agriculture before and after Photo-Oxidation. Polymers. 2020; 12: 753. https://doi.org/10.3390/polym12040753

[19] Qi Y, Li Y. Colorimetric Films Based on Polyvinyl Alcohol and Anthocyanins Extracted from Purple Tomato to Monitor the Freshness of Shrimp. Polymers. 2024; 16: 495. https://doi.org/10.3390/polym16040495

[20] Holman BWB, Bekhit AEDA, Waller M, Bailes KL, Kerr MJ, Hopkins DL. The association between total volatile basic nitrogen (TVB-N) concentration and other biomarkers of quality and spoilage for vacuum packaged beef. Meat Science. 2021; 179: 108551. https://doi.org/10.1016/j.meatsci.2021.108551

[21] Zhang R, Zhang P, Xia F, Jin Z, Chen S, Yu Y, et al. Preparation of chitosan photodynamic antibacterial film loaded with VK_3 complex in the preservation of chilled mutton. International Journal of Biological Macromolecules. 2024; 274: 133105. https://doi.org/10.1016/j.ijbiomac.2024.133105

[22] Chang H, Korma SA, Chen J, Yang T. Preparation, properties, and characterization of dual-modified tapioca starch and its composite film. Industrial Crops and Products. 2024; 222: 119840. https://doi.org/10.1016/j.indcrop.2024.119840

[23] Akhter R, Masoodi FA, Wani TA, Rather SA. Functional characterization of biopolymer based composite film: Incorporation of natural essential oils and antimicrobial agents. International Journal of Biological Macromolecules. 2019; 137: 1245–1255. https://doi.org/10.1016/j.ijbiomac.2019.06.214

[24] Bernad SI, Socoliuc V, Craciunescu I, Turcu R, Bernad ES. Field-Induced Agglomerations of Polyethylene-Glycol-Functionalized Nanoclusters: Rheological Behaviour and Optical Microscopy. Pharmaceutics. 2023; 15: 2612. https://doi.org/10.3390/pharmaceutics15112612

[25] Liu B, Gao J, Liu X, Zhang X, Zeng X, Zhang X, et al. Preparation of soybean isolate protein/xanthan gum/agar-Lycium ruthenicum anthocyanins intelligent indicator films and its application in mutton preservation. International Journal of Biological Macromolecules. 2024; 283: 137751. https://doi.org/10.1016/j.ijbiomac.2024.137751

[26] Lv Z, Meng X, Sun S, Jiang T, Zhang S, Feng J. Biodegradable Carboxymethyl Chitosan/Polyvinyl Alcohol Hymexazol-Loaded Mulch Film for Soybean Root Rot Control. Agronomy. 2023; 13: 2205. https://doi.org/10.3390/agronomy13092205

[27] Cui C, Gao L, Dai L, Ji N, Qin Y, Shi R, et al. Hydrophobic Biopolymer-Based Films: Strategies, Properties, and Food Applications. Food Engineering Reviews. 2023; 15: 360-379. https://doi.org/10.1007/s12393-023-09342-6

[28] Pires JRA, Souza VGL, Fuciños P, Pastrana L, Fernando AL. Methodologies to Assess the Biodegradability of Bio-Based Polymers-Current Knowledge and Existing Gaps. Polymers. 2022; 14: 1359. https://doi.org/10.3390/polym14071359

[29] Wang H, Han P, Zhao Y, Lu L, Qi W, Zhao K, et al. Preparation and characteristics of carboxymethyl cellulose-based films embedding cinnamon essential oil and their application on mutton preservation. Frontiers in Nutrition. 2025; 12: 1559833. https://doi.org/10.3389/fnut.2025.1559833

[30] Öncül N, Tokatli K, Yildirim Z. The inhibitory effect of lactococcin BZ against Escherichia coli on fresh beef. Journal of Food Safety and Food Quality. 2024; 75: 4–12. https://doi.org/10.53194/0003-925X-75-4

[31] International Commission on Microbiological Specifications for Foods (ICMSF). Microorganisms in Foods 2: Sampling for Microbiological Analysis: Principles and Specific Applications. 2nd edn. University of Toronto Press: Toronto. 1986. Available at: https://seafood.oregonstate.edu/sites/agscid7/files/snic/sampling-for-microbiological-analysis-principlesand-specific-applications-icmsf.pdf (Accessed: 4 August 2021).

[32] Farahmand Z, Terzi Gulel G. Investigation of the antibacterial effect of curcumin against Staphylococcus aureus in chicken meat. Journal of Food Safety and Food Quality. 2025; 76: 44343. https://doi.org/10.31083/JFSFQ44343